Comparison of Induction Machine Stator Vibration Spectra Induced by Reluctance Forces and Magnetostriction

Koen Delaere, Ward Heylen, Ronnie Belmans, and Kay Hameyer

***Abstract*—For rotating electric machines, the reluctance forces (Maxwell stresses) acting on the stator teeth are a major cause of noise emission. Next to the reluctance forces, magnetostriction is a potential cause of additional noise from electric machines. First, a thermal stress analogy is used to introduce magnetostriction in the finite-element framework. Next, we present the computation and comparison of the stator vibration spectra caused by these two effects separately, by example of a 45-kW induction machine. Moreover, two kinds of magnetostriction characteristics of the stator yoke material are compared: a quadratic $\lambda(B)$ curve and a $\lambda(B)$ curve with zero-crossing around 1.5 Tesla.**

***Index Terms*—Coupled magnetomechanical problems, finite-element methods, magnetostriction.**

I. Introduction

NOISE and vibration research has been focusing on reluctance forces (Maxwell stresses) as the major cause of noise and vibrations in rotating electric machinery. For nonrotating machinery (transformers, inductors), magnetostriction is the major cause of noise, but also for induction machines, magnetostriction can be responsible for a considerable part of the machine's noise [1], [2]. The simulation of vibration spectra induced by reluctance forces has been investigated extensively using finite-element models, e.g., [3] and [4], while the simulation of magnetostriction effects has been left aside. This is partly due to the fact that accurate magnetostriction data are hard to obtain. The magnetostriction of the yoke material also depends on its stress condition, but it is hard to estimate the stress remaining in the material after a shrink-fit of the yoke into the stator housing. Moreover, it is often difficult to embed this kind of material behavior in (existing) finite-element software, although this may be resolved with the advent of powerful methods like Preisach material modeling, which can be enhanced to encompass magnetostriction [5]. A straightforward finite-element method to capture the magnetostrictive deformation that is based upon a thermal stress analogy, has been presented earlier [6]. The theoretical background is repeated here briefly and is subsequently used to estimate, for a 45-kW induction machine:

1) the relative importance of reluctance forces and magnetostriction with respect to stator deformation;
2) the impact of using materials with different magnetostrictive behavior.

The isotropic magnetostriction curve

$$\lambda = 10^{-6}B^2 \tag{1}$$

will be referred to as *magnetostriction type 1* and the isotropic curve with zero-crossing around 1.5 tesla (T)

$$\lambda = 10^{-6}(B^2 - 0.4B^4) \tag{2}$$

will be referred to as *magnetostriction type 2*. Both kinds of magnetostriction occur commonly in electric steels. We confine ourselves to two-dimensional (2-D) models, but the concepts introduced here are easily extended to three-dimensional finite-element models.

II. Thermal Stress Analogy

For plane stress ($\sigma_z = 0$), the *elastic strain* in x direction $\varepsilon_{el,x}$ is determined by the external stresses σ_x and σ_y

$$\varepsilon_{el,x} = \frac{1}{E}(\sigma_x - \nu\sigma_y) \tag{3}$$

where E and ν are the Young and Poisson modulus, respectively. When a material with thermal expansion coefficient α_T is heated, it will exhibit a *thermal strain* $\alpha_T\Delta T$ which is added to the elastic strain $\varepsilon_{el,x}$ in order to give the total strain $\varepsilon_x = \varepsilon_{el,x} + \alpha_T\Delta T$. The elasticity equation (3) is now written as [7]

$$\varepsilon_x - \alpha_T\Delta T = \frac{1}{E}(\sigma_x - \nu\sigma_y). \tag{4}$$

The same procedure is valid for magnetostrictive strain $\lambda(B)$ instead of thermal strain, giving

$$\varepsilon_x - \lambda(B) = \frac{1}{E}(\sigma_x - \nu\sigma_y). \tag{5}$$

Manuscript received July 5, 2001; revised October 25, 2001. This work was supported by the "Fonds voor Wetenschappelijk Onderzoek Vlaanderen (FWOV)." This work was also supported by the Belgian Ministry of Scientific Research through granting the IUAP P4/20 on Coupled Problems in Electromagnetic Systems. The research Council of the K. U. Leuven supported numerical research. The work of K. Delaere was supported by a FWOV scholarship.

K. Delaere, R. Belmans, and K. Hameyer are with the Katholieke Universiteit Leuven, Department ESAT-ELEN, B3001 Leuven-Heverlee, Belgium (e-mail: kay.hameyer@esat.kuleuven.ac.be).

W. Heylen is with the Katholieke Universiteit Leuven, Department Mechanics-PMA, B3001 Leuven-Heverlee, Belgium (e-mail: ward.heylen@mech.kuleuven.ac.be).

Publisher Item Identifier S 0018-9464(02)02376-2.

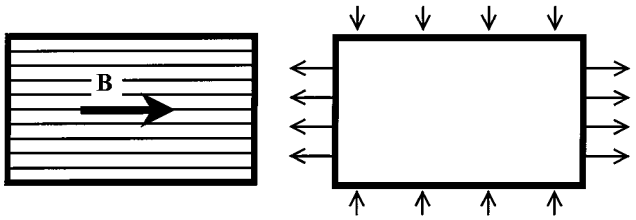

Fig. 1. The magnetostriction forces distribution (b) representing the strain caused by (a) magnetostriction due to the magnetic field $\mathbf{B}$, consists of a set of forces parallel to $\mathbf{B}$ and a set of forces perpendicular to $\mathbf{B}$.

Similarly, the elastic energy U of a mechanical finite-element system is determined by the *elastic displacement* a_{el} and the mechanical stiffness matrix K

$$U = \tfrac{1}{2}\, a_{el}^{\mathrm{T}} K a_{el} \tag{6}$$

where again the elastic displacement a_{el} is not necessarily equal to the total displacement a, since the material may exhibit thermal or magnetostrictive expansion. The elastic energy U expressed in terms of total displacement a and magnetostrictive displacement α_{ms} is

$$U = \tfrac{1}{2}\, (a - \alpha_{ms})^{\mathrm{T}} K (a - \alpha_{ms}). \tag{7}$$

The next section describes how the magnetostrictive displacement α_{ms} is found, and how this leads to the concept of magnetostriction forces, the latter being the direct equivalent of thermal stresses (Fig. 1).

III. Magnetostriction Forces

For finite-element models, the magnetostrictive displacement α_{ms} can be computed on an element-by-element basis. The midpoint (center of gravity) of the finite-element is held fixed. The magnetostrictive strain of the element is found using the element's flux density B^e and the $\lambda(B)$ characteristic of the material. If a set of $\lambda(B, \sigma)$ characteristics are given, one is chosen for the appropriate value of tensile stress.

A. Isotropic Magnetostriction

For materials with isotropic magnetostriction (Fig. 2), the local xy axis of the element are rotated in such a way that the flux density vector $\mathbf{B}$ coincides with the local x axis. The strains λ_x and λ_y in the local frame are then given by

$$\begin{aligned} \lambda_x &= \lambda \\ \lambda_y &= \lambda_t = -\lambda/2 \\ \lambda_z &= \lambda_t = -\lambda/2 \end{aligned} \tag{8}$$

where $\lambda = \lambda(B)$ is the magnetostrictive strain in the direction of $\mathbf{B}$ (x direction) and λ_t is the magnetostrictive strain in the transverse y and z directions. Usually, magnetostriction will leave the total volume and density unchanged [8], so that $\lambda_y = \lambda_z = -\lambda_x/2$. This volume invariance is equivalent to a magnetostrictive "Poisson modulus" of 0.5, which is bigger than the mechanical Poisson modulus of about 0.3. Therefore,

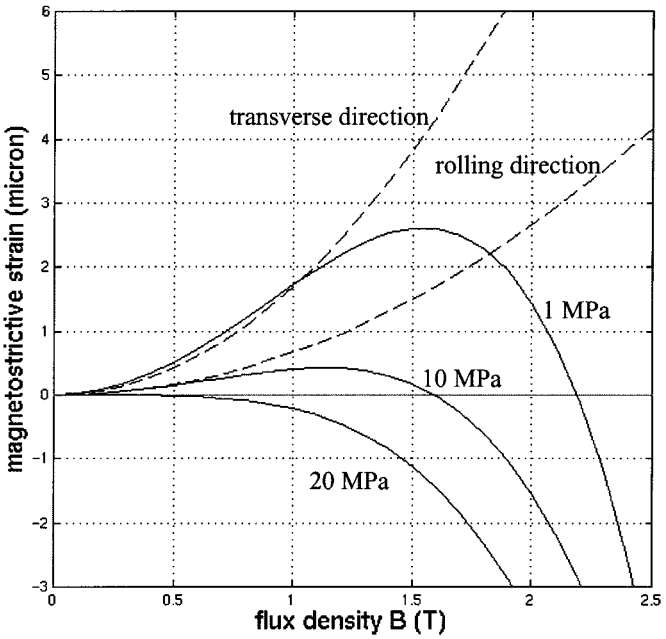

Fig. 2. Magnetostrictive material characteristics for isotropic nonoriented 3% SiFe (solid lines, as a function of tensile stress) and anisotropic M330-50A (dashed lines, for rolling and transverse direction).

when the magnetostrictive deformation is represented by a set of mechanical forces in the direction of the vector $\mathbf{B}$, there is always a set of forces perpendicular to $\mathbf{B}$ to correct this difference in Poisson modulus (Fig. 1). The above is valid for *plane stress*. In a 2-D *plane strain* analysis, the thickness (z direction) of the material has to remain constant and an additional tensile z stress needs to be applied in order to obtain $\lambda_z = 0$. This adjusts the values (8) to

$$\begin{aligned} \lambda_x &= \lambda + \nu\lambda_t \\ \lambda_y &= \lambda_t + \nu\lambda_t \\ \lambda_z &= \lambda_t - \lambda_t = 0 \end{aligned} \tag{9}$$

where ν is the mechanical Poisson modulus of the material and $\lambda_t = -\lambda/2$.

B. Anisotropic Magnetostriction

Fig. 2 shows a typical magnetostriction characteristic for anisotropic M330-50A steel (dashed lines) for rolling direction and transverse direction. As an approximation of the anisotropic behavior, the flux density vector is decomposed into a B_x and a B_y component in the element's local xy axis, arranged so that the x axis coincides with the rolling direction, and the y axis with the transverse direction. The rolling direction curve $\lambda_{\mathrm{RD}}(B)$ is then used with B_x as input, and the perpendicular direction curve $\lambda_{\mathrm{PD}}(B)$ with B_y as input, giving, for *plane stress*

$$\begin{aligned} \lambda_x &= \lambda_{\mathrm{RD}}(B_x) - \lambda_{\mathrm{PD}}(B_y)/2 \\ \lambda_y &= \lambda_{\mathrm{PD}}(B_y) - \lambda_{\mathrm{RD}}(B_x)/2 \\ \lambda_z &= -\lambda_{\mathrm{RD}}(B_x)/2 - \lambda_{\mathrm{PD}}(B_y)/2. \end{aligned} \tag{10}$$

Depending on the actual anisotropic behavior of the material, a more accurate strain description can be used, e.g., taking magnetostrictive shear λ_{xy} into account [9]. A similar correction as in (9) can be made for the *plane strain* case.

C. Magnetostrictive Displacement α_{ms}

Still working in the local xy axis, the strains λ_x, λ_y are now converted into nodal displacements $\alpha^e_{ms} = (\alpha^e_{x,\,i},\, \alpha^e_{y,\,i})$ considering the midpoint of the element $(x_m,\, y_m)$ as fixed

$$\begin{bmatrix} \alpha^e_{x,\,i} \\ \alpha^e_{y,\,i} \end{bmatrix} = \begin{bmatrix} (x_i - x_m)\lambda_x \\ (y_i - y_m)\lambda_y \end{bmatrix}, \qquad i = 1,\, 2,\, 3 \tag{11}$$

where i indicates the element nodes with coordinates $(x_i,\, y_i)$.

D. Magnetostriction Forces F_{ms}

The mechanical stiffness matrix K^e for one element gives, after multiplication with the magnetostrictive displacement α^e_{ms} of the nodes, the nodal *magnetostriction forces*

$$F^e_{ms} = K^e \alpha^e_{ms}. \tag{12}$$

Equation (12) has to be performed element by element (using K^e) and not for the whole mesh at once (using the global matrix K). This is because the N different displacements $\alpha_{ms,\,j}$, $j = 1 \cdots N$, due to magnetostriction in the N elements surrounding one specific node, should *not* be summed. These N displacements $\alpha_{ms,\,j}$ should first be converted into magnetostriction forces, and then the N forces are summed to give the total force on this node.

When the magnetostriction forces for all elements have been computed, they are summed to give the total magnetistriction force distribution F^{ms}

$$F_{ms} = \sum_e F^e_{ms}. \tag{13}$$

Fig. 1(b) shows the resulting F_{ms} for a square block of material subject to a homogeneous field; all internal node forces cancel. Once this distribution is known, the corresponding global deformation a_{ms} of the entire structure due to magnetostriction, is found using the global mechanical stiffness matrix K

$$K a_{ms} = F_{ms}. \tag{14}$$

Note that (13) should only be used to find F^e_{ms} from α^e_{ms}, while (14) should only be used to find a_{ms} from F_{ms}. Since the global stiffness matrix K was used to find a_{ms}, the influence of external boundary conditions has been taken into account, as well as the effect of the shape of the body (e.g., ring-shaped stator).

IV. Magnetomechanical System

The total energy E of the magnetomechanical system is the sum of the elastic energy U and the magnetic energy W

$$E = U + W = \tfrac{1}{2}\, a^{\mathrm{T}}_{el} K a_{el} + \tfrac{1}{2}\, A^{\mathrm{T}} M A \tag{15}$$

where M is the magnetic stiffness matrix and A is the z-component of magnetic vector potential. The mechanical equation of the magnetomechanical system is found by considering the virtual work done by a set of external forces R (where vector potential A remains constant)

$$\frac{\partial E}{\partial a} = \frac{\partial U}{\partial a} + \frac{\partial W}{\partial a} = R. \tag{16}$$

The magnetic forces (reluctance forces as well as Lorentz forces [6]) are found by the virtual work term [10]

$$F_{mag} = -\frac{\partial W}{\partial a} = -\int_0^A A^{\mathrm{T}}\, \frac{\partial M}{\partial a}\, dA \tag{17}$$

which is valid for linear and nonlinear magnetic systems. The elastic forces as well as the magnetostriction forces are given by the other virtual work term $\partial U/\partial a$. First, we write the elastic energy as the sum of all element contributions

$$U = \sum_e \tfrac{1}{2}\, (a^e_{el})^{\mathrm{T}} K^e a^e_{el} \tag{18}$$

then, using $a^e_{el} = a^e - \alpha^e_{ms}$, the partial derivative $\partial U/\partial a$ becomes

$$\frac{\partial U}{\partial a} = \sum_e \frac{\partial (a^e_{el})^{\mathrm{T}}}{\partial a} K^e a^e_{el} \tag{19}$$

$$= \sum_e K^e (a^e - \alpha^e_{ms}) \tag{20}$$

$$= K a - F_{ms} \tag{21}$$

since $\partial a_{el}/\partial a = 1$ for constant A. When the feedback of magnetostriction on the magnetic field is neglected, the magnetic equation of the magnetomechanical system is just $MA = T$, where T is the source term vector. The magnetomechanical system then becomes

$$\begin{bmatrix} M & 0 \\ 0 & K \end{bmatrix} \begin{bmatrix} A \\ a \end{bmatrix} = \begin{bmatrix} T \\ R + F_{mag} + F_{ms} \end{bmatrix} \tag{22}$$

where the second equation is obtained by substituting (17) and (21) into (16). The system (22) can be solved in a numerically weak coupled scheme, first solving the magnetic problem and then solving for the mechanical displacement.

V. Modal Decomposition

The vibration of the stator is governed by

$$M_m \ddot{a} + C_m \dot{a} + K a = f(t) \tag{23}$$

where $a(t)$ is the nodal displacement vector and $f(t)$ is the force distribution acting on the stator for a specific rotor position α, $f(t) = f^{\alpha}$. M_m, C_m, and K are the mechanical mass, damping, and stiffness matrices. Neglecting damping ($C_m = 0$) and using the modal decomposition $a = Pq$ with P the modal matrix containing a selected set of $N = 30$ stator mode shapes, and q the vector of generalized modal coordinates, (23) is transformed into [11]

$$\ddot{q}_i + \omega_i^2 q_i = \Gamma_i(t), \qquad i = 1 \cdots N \tag{24}$$

where ω_i is the mode's eigenfrequency. The modes are calculated taking mass and stiffness of both the yoke iron and the stator coil copper into account. For a given force pattern f^{α} (in

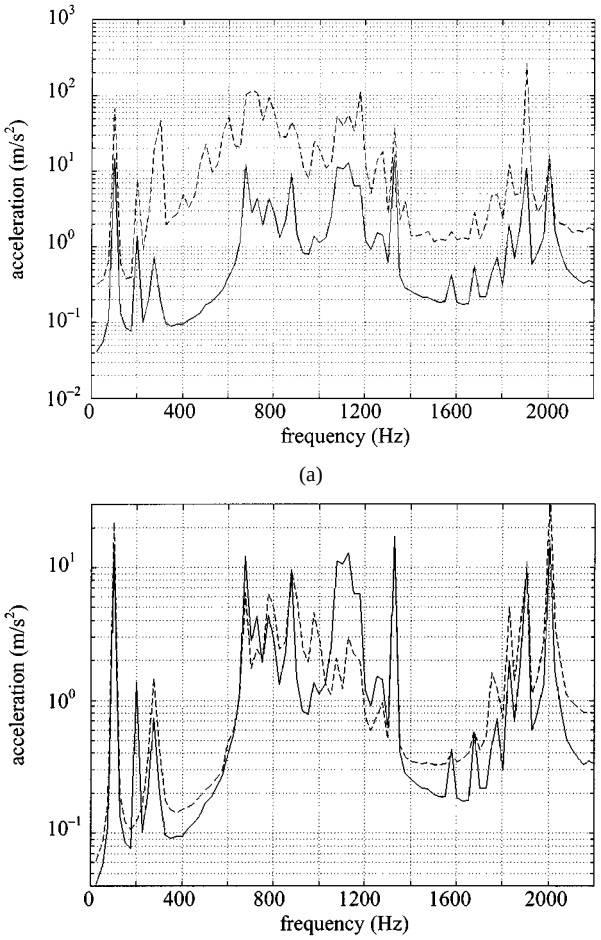

Fig. 3. Stator acceleration spectra induced by (a) reluctance forces (dotted line) and magnetostriction type 2 (solid line), (b) magnetostriction type 1 (dotted line) and magnetostriction type 2 (solid line).

this case F_{mag} or F_{ms}) occurring for rotor position α, and a given mode shape ϕ_i, the mode participation factor (MPF) Γ_i^α is

$$\Gamma_i^\alpha = \frac{\phi_i^T f^\alpha}{\phi_i^T M_m \phi_i}. \tag{25}$$

For a slip s, the period of the MPF can be approximated by $90°/(1-s) = 88.66°$ or a multiple of this [4]. Here, the period of the MPF is approximated by $360°/(1-s) = 354.6°$ and the MPF are sampled using 180 rotor positions at 2° intervals. From (25), the MPF are known as a function of rotor position, and the rotor speed n allows us to find the MPF as a function of time. The individual modal equations are solved in the frequency domain by applying a discrete Fourier transformation to (24)

$$Q_i(k\Delta\omega) = \frac{\Gamma_i(k\Delta\omega)}{\omega_i^2 - (k\Delta\omega)^2}. \tag{26}$$

The spectrum Q_i of all mode shapes of interest can be found in this way. The separate complex spectra Q_i of the N relevant modes are composed back into the actual stator displacement and acceleration spectra using the modal composition $a = Pq$.

VI. Example: 45-kW Induction Machine

Fig. 3 compares the stator acceleration spectra computed for reluctance forces as well as for the two types of magnetostriction (1) and (2), for the case of a 45-kW induction machine under normal operation. Fig. 3(a) compares the stator acceleration spectra induced by reluctance forces (dotted line) and magnetostriction type 2 (solid line), while Fig. 3(b) compares the vibration spectrum induced by magnetostriction type 1 (dotted line) and magnetostriction type 2 (solid line). It can be seen that the vibrations (and, thu,s also the noise) due to magnetostriction are considerably smaller than the effect due to reluctance forces, except for the 100–Hz force component, where they are of the same order of magnitude. The overall difference between magnetostriction type I and II is small, and is only important for a few specific modes. The full analysis required 15 hours of CPU time on a HP-B1000 workstation.

VII. Conclusion

Using a thermal stress analogy, a set of magnetostriction forces is computed that induces the same strain in the material as magnetostriction does. Using the example of a 45-kW induction machine, this magnetostriction force distribution is compared to the reluctance force distribution with respect to the resulting stator vibration spectrum for two typical magnetostriction characteristics.

References

[1] L. Låftman, "The contribution to noise from magnetostriction and PWM inverter in an induction machine," Ph.D. dissertation, Dept. Ind. Elect. Eng, Automation, Lund Inst. Technol., KF Sigma, Lund, Sweden, 1995.
[2] G. Porges, *Appl. Acoust.*. London: Arnold, 1977.
[3] C. G. C. Neves, R. Carlson, N. Sadowski, J. P. A. Bastos, N. S. Soeiro, and S. N. Y. Gerges, "Experimental and numerical analysis of induction motor vibrations," presented at the CEFC 1998, Tucson, AZ.
[4] K. Delaere, A. Tenhunen, W. Heylen, K. Hameyer, and R. Belmans, "Predicting the stator vibration spectrum of induction machines under normal operation," presented at the INTERNOISE 1999, Fort Lauderdale, FL, 1999.
[5] A. Reimers and E. Della Torre, "Fast Preisach based magnetostriction model for highly magnetostrictive materials," *IEEE Trans. Magn.*, pt. 1, vol. 35, no. 3, pp. 1239–1242, May 1999.
[6] K. Delaere, W. Heylen, R. Belmans, and K. Hameyer, "Finite element based expression for Lorentz, Maxwell and magnetostriction forces," *Int. J. Computation Math. Elect. Electron. Eng. (COMPEL)*, vol. 20, no. 1, pp. 20–31, 2001.
[7] S. Timoshenko and J. N. Goodier, *Theory of Elasticity*: McGraw-Hill, 1951.
[8] D. Jiles, *Introduction to Magnetism and Magnetic Materials*. London, U.K.: Chapman & Hall, 1991.
[9] H. Pfützner and A. Hasenzagl, "Fundamental aspects of rotational magnetostriction," in *Nonlinear Electromagnetic Systems*, A. J. Moses and A. Basak, Eds. Cardiff, U.K.: IOS, 1996, pp. 374–379.
[10] J. L. Coulomb and G. Meunier, "Finite element implementation of virtual work principle for magnetic or electric force or torque computation," *IEEE Trans. Magn.*, vol. MAG-20, pp. 1894–1896, May 1984.
[11] W. T. Thomson, *Theory of Vibrations With Applications*, 4th ed. Englewood Cliffs, NJ: Prentice-Hall, 1993.